

Electromagnetic Interference in RIS-Aided Communications

Andrea de Jesus Torres, Luca Sanguinetti, *Senior Member, IEEE*, Emil Björnson, *Senior Member, IEEE*

Abstract—The prospects of using a reconfigurable intelligent surface (RIS) to aid wireless communication systems have recently received much attention. Among the different use cases, the most popular one is where each element of the RIS scatters the incoming signal with a controllable phase-shift, without increasing its power. In prior literature, this setup has been analyzed by neglecting the electromagnetic interference, consisting of the inevitable incoming waves from external sources. In this letter, we provide a physically meaningful model for the electromagnetic interference that can be used as a baseline when evaluating RIS-aided communications. The model is used to show that electromagnetic interference has a non-negligible impact on communication performance, especially when the size of the RIS grows large. When the direct link is present (though with a relatively weak gain), the RIS can even reduce the communication performance. Importantly, it turns out that the SNR grows quadratically with the number of RIS elements only when the spatial correlation matrix of the electromagnetic interference is asymptotically orthogonal to that of the channel vector towards the intended receiver. Otherwise, the SNR only increases linearly.

Index Terms—Reconfigurable intelligent surface, electromagnetic interference modelling, scattering environments.

I. INTRODUCTION

Reconfigurable intelligent surface (RIS) is an umbrella term used for a two-dimensional array of passive elements that will (diffusely) reflect incident electromagnetic waves after “passive” analog filtering [1]–[3]. Each element filters the signal by potentially reducing the amplitude, incurring time delays, and/or changing the polarization [4]. A basic use case of the RIS technology is illustrated in Fig. 1, where an RIS is deployed to capture signal energy from the source proportional to its area and re-radiate it in the shape of a beam towards the intended receiver. Since the RIS is not amplifying the signal, a large surface area is typically required to achieve a given signal-to-noise ratio (SNR) at the receiver.

RIS-aided communications is an emerging topic that is receiving a lot of attention [5] and several papers have identified potential benefits in terms of spectral efficiency [6] and energy efficiency [7]. However, a common practice is to only consider the signals generated by the system and thereby neglecting the electromagnetic interference (EMI) or “noise” (or “pollution”) that is inevitably present in any environment [8], [9]. The EMI may arise from a variety of natural, intentional or non-intentional causes; for example, man-made devices and natural background radiation. Largely speaking, any *uncontrollable* wireless signal produces EMI. Despite existing in any wireless communication system, it may have a severe effect in the

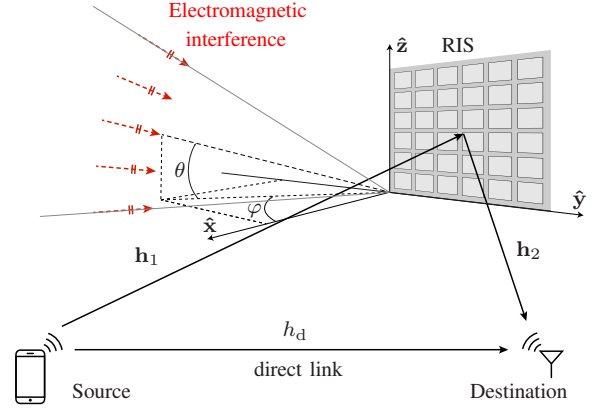


Fig. 1. RIS-aided communication system.

setup of Fig. 1 since the EMI that impinges on the RIS, from arbitrary spatial directions, is captured with an energy that is proportional to its area and then re-radiated. While the direction of the re-radiated EMI might not be focused at the intended receiver, a significant portion (due to the large surface area of the RIS) of its energy might reach it and, thus, degrade the end-to-end SNR of the system, which is typically designed for optimal performance in presence of only thermal noise.

In this letter, we present a physically meaningful model for the EMI that is produced by uncontrollable sources in the far-field of the RIS. The model is valid for arbitrary scattering and can be used as a baseline for the analysis and design of RIS-aided communications. Particularly, it is used to show that in a random scattering environment, the EMI may have a severe impact on the SNR, especially when the size of the RIS grows large. Importantly, it turns out that the SNR grows linearly, not quadratically as in [6], with the number of RIS elements. When a direct link with a relatively weak gain is present, the RIS can even reduce the communication performance.

II. SYSTEM MODEL

Consider a single-antenna transmitter communicating wirelessly with a single-antenna receiver in a scattering environment, while being aided by an RIS equipped with N reconfigurable elements. The N RIS elements are deployed on a two-dimensional square grid [1]. The setup is illustrated in Fig. 1 in a three-dimensional (3D) space, where a local spherical coordinate system is defined at the RIS with φ being the azimuth angle and θ being the elevation angle. We assume each element has an area A . The elements of the RIS are deployed edge-to-edge so the total area is NA . The elements are indexed row-by-row by $n \in [1, N]$, thus the n th element for $n = 1, \dots, N$ is located at $\mathbf{u}_n = [u_{x,n}, u_{y,n}, 0]^T$ where

$$u_{x,n} = -\frac{(\sqrt{N}-1)\sqrt{A}}{2} + \sqrt{A} \bmod (n-1, \sqrt{N}) \quad (1)$$

$$u_{y,n} = \frac{(\sqrt{N}-1)\sqrt{A}}{2} - \sqrt{A} \left\lfloor \frac{n-1}{\sqrt{N}} \right\rfloor. \quad (2)$$

L. Sanguinetti was supported by the Italian Ministry of Education and Research (MIUR) in the framework of the CrossLab project (Departments of Excellence). E. Björnson was supported by the FFL18-0277 grant from the Swedish Foundation for Strategic Research.

A. De Jesus Torres and L. Sanguinetti are with the University of Pisa, Dipartimento di Ingegneria dell'Informazione, 56122 Pisa, Italy (luca.sanguinetti@unipi.it). E. Björnson is with the Department of Computer Science, KTH Royal Institute of Technology, 10044 Stockholm, Sweden, and Linköping University, 58183 Linköping, Sweden (emilbjo@kth.se).

The channel vector between the source and RIS is called $\mathbf{h}_1 = [h_{1,1}, \dots, h_{1,N}]^T \in \mathbb{C}^N$ and the channel vector between the RIS and receiver is $\mathbf{h}_2 = [h_{2,1}, \dots, h_{2,N}]^T \in \mathbb{C}^N$. The configuration of the RIS is determined by the diagonal matrix $\mathbf{\Theta} = \mathbf{\Gamma}\mathbf{\Phi}$ with $\mathbf{\Gamma} = \text{diag}(\gamma_1, \dots, \gamma_N)$ and $\mathbf{\Phi} = \text{diag}(e^{-j\phi_1}, \dots, e^{-j\phi_N})$. Here, $\gamma_1, \dots, \gamma_N \in (0, 1]$ are the amplitude scattering variables (describing the fraction of the incident signal power that is scattered) and $\phi_1, \dots, \phi_N \in [0, 2\pi)$ are the phase-shift variables (describing the delays of the scattered signals).

A. Signal Model

The received signal $\mathbf{x} \in \mathbb{C}^N$ at the RIS is

$$\mathbf{x} = \mathbf{h}_1 s + \mathbf{n} \quad (3)$$

where s is the transmitted symbol with power $P = \mathbb{E}\{|s|^2\}$ and $\mathbf{n} \in \mathbb{C}^N$ is the EMI, produced by the incoming, uncontrollable electromagnetic waves. The received signal $y \in \mathbb{C}$ at the destination in Fig. 1 is

$$y = \mathbf{g}_2^H \mathbf{x} + h_d s + w \quad (4)$$

where $\mathbf{g}_2 = \mathbf{\Theta}^H \mathbf{h}_2$ is the effective channel, $h_d \in \mathbb{C}$ is the channel gain of the direct path, and $w \sim \mathcal{N}_{\mathbb{C}}(0, \sigma_w^2)$ is the thermal receiver noise. Plugging (3) into (4) yields

$$y = (\mathbf{g}_2^H \mathbf{h}_1 + h_d) s + \mathbf{g}_2^H \mathbf{n} + w. \quad (5)$$

The objective of this letter is to evaluate the impact of the EMI (or electromagnetic noise) \mathbf{n} on communication performance, which is neglected in the RIS literature. A statistical model is derived next based on electromagnetic principles.

B. Electromagnetic Interference Modeling

The EMI \mathbf{n} is produced by a superposition of continuum of incoming plane waves that are generated by external sources.¹ Suppose the waves are generated in the far-field of the half-space in front of the RIS. Each electromagnetic wave can thus be modeled as a plane wave that reaches the RIS from a particular azimuth angle $\varphi \in [-\pi/2, \pi/2)$ and elevation angle $\theta \in [-\pi/2, \pi/2)$; see Fig. 1. The EMI field \mathbf{n} is thus (e.g., [10])

$$\mathbf{n} = \iint_{-\pi/2}^{\pi/2} \mathbf{n}(\varphi, \theta) d\varphi d\theta \quad (6)$$

where $\mathbf{n}(\varphi, \theta) \in \mathbb{C}^N$ has entries

$$n_n(\varphi, \theta) = a(\varphi, \theta) e^{j\mathbf{k}(\varphi, \theta)^T \mathbf{u}_n}. \quad (7)$$

In (7), $\mathbf{k}(\varphi, \theta) \in \mathbb{R}^3$ is the wave vector

$$\mathbf{k}(\varphi, \theta) = \frac{2\pi}{\lambda} [\cos(\theta) \cos(\varphi), \cos(\theta) \sin(\varphi), \sin(\theta)]^T \quad (8)$$

that describes the phase variation of the plane wave with respect to the three Cartesian coordinates at the receiving volume, and $a(\varphi, \theta)$ is a zero-mean, complex-Gaussian random process with

$$\mathbb{E}\{a(\varphi, \theta) a(\varphi', \theta')\} = A \sigma^2 f(\varphi, \theta) \delta(\varphi - \varphi') \delta(\theta - \theta') \quad (9)$$

¹Note that even a single spherical wave can be expanded as a continuum of plane waves.

where $\sigma^2 f(\varphi, \theta)$ denotes the angular density of the interference power with $\iint_{-\pi/2}^{\pi/2} f(\varphi, \theta) d\varphi d\theta = 1$. From (6), using (7) and (9) yields

$$\mathbb{E}\{\mathbf{n}\mathbf{n}^H\} = A \sigma^2 \mathbf{R} \quad (10)$$

with

$$[\mathbf{R}]_{n,m} = \iint_{-\pi/2}^{\pi/2} e^{j\mathbf{k}(\varphi, \theta)^T (\mathbf{u}_n - \mathbf{u}_m)} f(\varphi, \theta) d\varphi d\theta. \quad (11)$$

The following model is thus valid for any arbitrary $f(\varphi, \theta)$.

Corollary 1. *The EMI \mathbf{n} is distributed as*

$$\mathbf{n} \sim \mathcal{N}_{\mathbb{C}}(\mathbf{0}, A \sigma^2 \mathbf{R}) \quad (12)$$

where the (n, m) th element of \mathbf{R} is given by (11).

Notice that

$$\frac{1}{N} \text{tr}(\mathbf{R}) = \iint_{-\pi/2}^{\pi/2} f(\varphi, \theta) d\varphi d\theta = 1. \quad (13)$$

Although valid for any arbitrary $f(\varphi, \theta)$, the nature of the EMI makes it reasonable to assume that the electromagnetic waves are impinging from directions spanning a large angular interval. In the case of a uniform distribution from all angles (i.e., isotropic conditions), (11) reduces to [11, Prop. 1]

$$[\mathbf{R}]_{n,m} = \text{sinc}\left(\frac{2\|\mathbf{u}_n - \mathbf{u}_m\|}{\lambda}\right) \quad (14)$$

where $\|\cdot\|$ denotes the Euclidean norm.

Remark 1. *In wireless communications, the noise is usually modeled as independent circularly-symmetric Gaussian random variables, i.e., $\mathbf{R} = \mathbf{I}_N$. However, this is never the case for the noise (interference) samples of electromagnetic nature that interact with an RIS, as can be seen from (11). Even in the special case of an isotropic angular distribution, (14) shows that $\mathbf{R} = \mathbf{I}_N$ only when $\|\mathbf{u}_n - \mathbf{u}_m\| = i\lambda/2$, with $i \in \mathbb{Z}$, i.e., all the RIS elements are positioned along a straight line at a spacing of an integer multiple of $\lambda/2$. This can never happen with a two-dimensional RIS.*

C. Channel Modeling

The channels \mathbf{h}_1 , \mathbf{h}_2 , and h_d can be either deterministic or stochastic depending on the propagation conditions. The simplest deterministic model is obtained by assuming that the source and destination are in the far-field of the RIS and a single line-of-sight path is present. We call φ_i and θ_i the azimuth and elevation angles of the single path for the two links in Fig. 1, for $i = 1, 2$. In this case, we have that

$$h_{1,n} = \sqrt{A\beta_1} e^{j\mathbf{k}(\varphi_1, \theta_1)^T \mathbf{u}_n} \quad (15)$$

$$h_{2,n} = \sqrt{A\beta_2} e^{j\mathbf{k}(\varphi_2, \theta_2)^T \mathbf{u}_n} \quad (16)$$

with $|h_{1,n}|^2 = A\beta_1$ and $|h_{2,n}|^2 = A\beta_2$ for $n = 1, \dots, N$. The direct path $h_d \in \mathbb{C}$ is such that $|h_d|^2 = \beta_d$. In a random scattering environment, $\mathbf{h}_1, \mathbf{h}_2$ are independent and distributed as [11, Cor. 1])

$$\mathbf{h}_i \sim \mathcal{N}_{\mathbb{C}}(\mathbf{0}, A\beta_i \mathbf{R}_i) \quad i = 1, 2 \quad (17)$$

where the (n, m) th element of \mathbf{R}_i is given by (11) with power spectral density $f_i(\varphi, \theta)$. The direct path h_d has a Rayleigh fading distribution $h_d \sim \mathcal{N}_{\mathbb{C}}(0, \beta_d)$, where β_d is the variance.

III. PERFORMANCE ANALYSIS

Assume that perfect channel knowledge is available in the system. From (5), the SNR at the destination is

$$\text{SNR} = \frac{P|\mathbf{g}_2^H \mathbf{h}_1 + h_d|^2}{A\sigma_w^2 \mathbf{g}_2^H \mathbf{R} \mathbf{g}_2 + \sigma_w^2} \quad (18)$$

$$= \frac{1}{\frac{A\sigma_w^2}{\sigma_w^2} \mathbf{g}_2^H \mathbf{R} \mathbf{g}_2 + 1} \frac{P}{\sigma_w^2} |\mathbf{g}_2^H \mathbf{h}_1 + h_d|^2. \quad (19)$$

With the optimal phase-configuration against thermal noise, e.g., [12], [13], we have that $\phi_n = \arg(h_{1n}h_{2n}) - \arg(h_d)$ and (18) becomes

$$\text{SNR} = \frac{1}{\frac{A\sigma_w^2}{\sigma_w^2} \mathbf{g}_2^H \mathbf{R} \mathbf{g}_2 + 1} \overline{\text{SNR}} \quad (20)$$

where

$$\overline{\text{SNR}} = \frac{P}{\sigma_w^2} \left(\sum_{n=1}^N \gamma_n |h_{1n}h_{2n}| + |h_d| \right)^2 \quad (21)$$

is the maximized SNR in absence of EMI [12], [13]. The impact of the EMI is next quantified under different conditions.

A. Without the Direct Link

We start by analyzing the case without the direct link, i.e., $\beta_d = 0$ ($-\infty$ dB). Following [11], we consider a setup in which $P/\sigma_w^2 = 124$ dB and the channels $\mathbf{h}_1, \mathbf{h}_2$ are isotropic with $\beta_1 = \beta_2 = -55$ dB and $A = (\lambda/4)^2$ with $\lambda = 0.1$. The EMI is also modeled as isotropic. We assume $\gamma_1 = \dots = \gamma_N = 1$. Fig. 2 shows the optimized SNR (20) as a function of N when $\sigma^2 = -50, -60$, and -70 dB. The curves show the median value and the bars indicate the interval where 90% of the random realizations appears. The impact of EMI depends on whether it is larger than the 1-term in the denominator of (20). The impact is small when it is close to one. In the investigated scenarios, we see that the EMI has a non-negligible effect on the SNR already when $\sigma^2 = -70$ dB, which is 15 dB lower than β_1 and β_2 . The gap increases as σ^2 increases but also when N grows large. This is a very undesirable effect since a physically large RIS is needed to compensate for the propagation losses and thereby increase SNR in (21).

B. With the Direct Link

We now consider a simulation scenario in which the direct path is present. Fig. 3 shows the optimized SNR in (20) for the same setup as in Fig. 2 with $\sigma^2 = -60$ dB, but with $\beta_d = -130$ dB and -120 dB. The curves 'w/o RIS' refer to the SNR achieved without the aid of the RIS. We notice that the RIS can increase the SNR by orders-of-magnitude when the EMI is neglected. However, when it is considered, the gain reduces substantially when $\beta_d = -130$ dB. Interestingly, the RIS even deteriorates the performance when the direct path gain is $\beta_d = -120$ dB, which is relatively weak (compared to

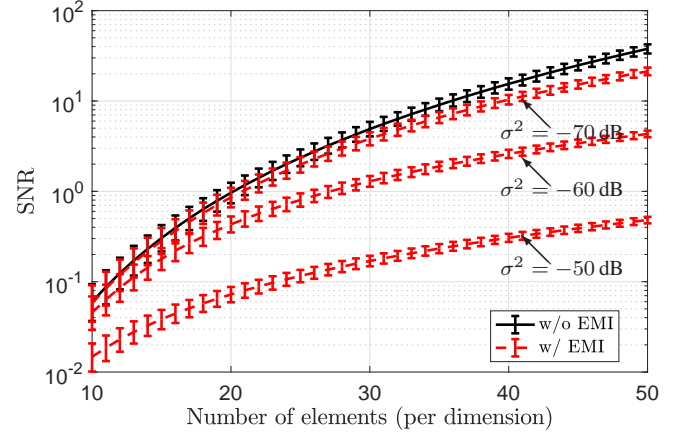


Fig. 2. The SNR achieved with an optimized RIS without the direct path for varying N with EMI. The performance achieved without EMI is reported as a reference. An isotropic scattering is considered for \mathbf{n} and $\{\mathbf{h}_i\}$ for $i = 1, 2$.

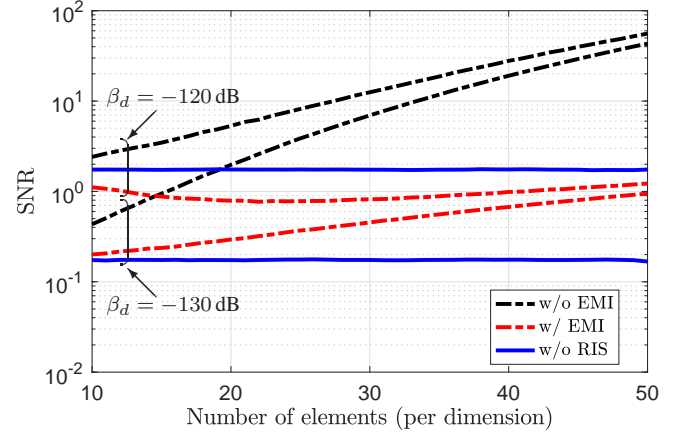


Fig. 3. The SNR achieved with an optimized RIS for varying N with the direct path in the presence of isotropic scattering for \mathbf{n} and $\{\mathbf{h}_i\}$ for $i = 1, 2$.

$\beta_1 = \beta_2 = -55$ dB) and likely present in practical situations. The negative impact of having the RIS increases if β_d grows. This is because when the direct link is present, a large number of elements N is needed if the extra signal power delivered by the RIS should make a difference in the SNR calculation. However, the extra interference (or noise) that is reflected by the RIS can dominate over the thermal noise in the receiver even when the RIS is relatively small, thereby reducing the SNR. This makes it evident that the EMI plays a key role in RIS-aided communications.

C. Power Scaling Law With Infinitely Large RIS

The results in Figs. 2 and 3 show that the scaling behavior of the SNR is much different with or without the EMI. Hence, we now study the asymptotic SNR (20) when $N \rightarrow \infty$. To this end, we recall the following result.

Lemma 1. [11, Prop. 2] In a scattering environment with \mathbf{h}_1 and \mathbf{h}_2 being independent and distributed as in (17), we have

that, as $N \rightarrow \infty$,

$$\frac{\overline{\text{SNR}}}{N^2} \xrightarrow{p} \frac{P}{\sigma_w^2} \beta_1 \beta_2 \left(\frac{\pi}{4} A \right)^2 \quad (22)$$

where convergence is in probability.

Lemma 1 implies that the SNR in the absence of EMI scales quadratically as N grows large. This is an instance of the so-called “square law” property of RIS-aided communications, originally presented in [5], [14] and commonly adopted in the RIS literature. To derive the power scaling law with EMI, we make the following technical assumptions:

Assumption 1. $\liminf_N \frac{1}{N} \text{tr}(\mathbf{R}) > 0$, $\limsup_N \|\mathbf{R}\|_2 < \infty$.

Assumption 2. For $i = 1, 2$ $\liminf_N \frac{1}{N} \text{tr}(\mathbf{R}_i) > 0$, $\limsup_N \|\mathbf{R}_i\|_2 < \infty$.

Proposition 1. Assume a scattering environment with \mathbf{h}_1 and \mathbf{h}_2 being independent and distributed as in (17). If Assumptions 1 and 2 hold and

$$\liminf_N \frac{1}{N} \text{tr}(\mathbf{R}_2 \mathbf{R}) > 0 \quad (23)$$

then, as $N \rightarrow \infty$,

$$\frac{\text{SNR}}{N} \xrightarrow{p} \frac{P}{\sigma^2} \frac{\beta_1}{\alpha} \left(\frac{\pi}{4} \right)^2 \quad (24)$$

where $\alpha = \lim_N \frac{1}{N} \text{tr}(\mathbf{R}_2 \mathbf{\Gamma} \mathbf{R} \mathbf{\Gamma})$ and convergence is in probability.

Proof: After dividing both sides by N , (20) reduces to (multiplying and dividing the left-hand-side by N)

$$\frac{\text{SNR}}{N} = \frac{1}{\frac{A\sigma^2}{\sigma_w^2} \frac{1}{N} \mathbf{g}_2^H \mathbf{R} \mathbf{g}_2 + \frac{1}{N}} \frac{\overline{\text{SNR}}}{N^2}. \quad (25)$$

We recall that $\mathbf{g}_2 = \mathbf{\Theta}^H \mathbf{h}_2 = \mathbf{\Gamma}^H \mathbf{\Phi}^H \mathbf{h}_2$ (after exchanging $\mathbf{\Phi}$ and $\mathbf{\Gamma}$ because they are diagonal). We notice that \mathbf{h}_2 and $\mathbf{\Phi}^H \mathbf{h}_2$ are statistically equivalent since $\mathbf{\Phi}$ is a diagonal phase-shift matrix. By applying [15, Th. 3.4], we have that, as $N \rightarrow \infty$,²

$$\frac{1}{N} \mathbf{g}_2^H \mathbf{R} \mathbf{g}_2 \xrightarrow{\text{a.s.}} A \beta_2 \alpha \quad (26)$$

almost surely.³ By using the continuous mapping theorem [15], it thus follows that the first term in (25) converges almost surely to $\sigma_w^2 / (\sigma^2 \beta_2 \alpha)$. Since almost sure convergence implies convergence in probability, the result in (24) follows since we know from Lemma 1 that $\overline{\text{SNR}}/N^2$ converges to (22) in probability. ■

Proposition 1 shows that the SNR scales linearly, not quadratically, as N grows large. The signal power grows as N^2 but is divided by the EMI, which grows as N , plus the thermal noise that is independent of N . Technically speaking, the new scaling behavior is a direct consequence of the condition (23), which states that \mathbf{R}_2 and \mathbf{R} are *not asymptotically orthogonal*, as $N \rightarrow \infty$. This implies that Proposition 1 is valid as long as the common subspace of the matrices \mathbf{R}_2 and \mathbf{R} has a

²Under Assumptions 1 and 2, it can be proved that $\mathbf{R}_2 \mathbf{\Gamma} \mathbf{R} \mathbf{\Gamma}$ is uniformly bounded and $\limsup_N \frac{1}{N} \text{tr}(\mathbf{R}_2 \mathbf{\Gamma} \mathbf{R} \mathbf{\Gamma}) < \infty$.

³Notice that if (23) is valid, then $\liminf_N \alpha > 0$ since $\mathbf{\Gamma} = \text{diag}(\gamma_1, \dots, \gamma_N)$ with $\gamma_1, \dots, \gamma_N \in (0, 1]$.

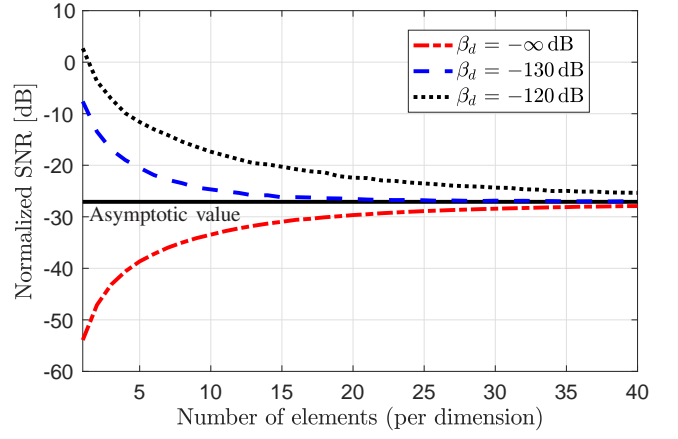


Fig. 4. Scaling behavior of the optimized SNR, normalized to N , as a function of N for different values of β_d and isotropic scattering conditions for \mathbf{n} and $\{\mathbf{h}_i\}$ for $i = 1, 2$.

dimension and eigenvalues that grow linearly with N [16]. In the case when (23) does not hold true, that is, \mathbf{R}_2 is asymptotically orthogonal to \mathbf{R} , i.e., $\frac{1}{N} \text{tr}(\mathbf{R}_2 \mathbf{R}) \rightarrow 0$ as $N \rightarrow \infty$, then the effect of the EMI vanishes and the SNR grows quadratically with $N \rightarrow \infty$. Although possible, this is unlikely to happen in practice since the EMI accounts for uncontrollable electromagnetic waves that can impinge on the RIS from arbitrary (and many) spatial directions. Therefore, in Figs. 2 and 3, the SNR reduction due to the EMI only represents the gap for a given number of elements, while the asymptotic gap grows without bound if (23) is satisfied.

Fig. 4 illustrates the behavior of SNR/N for varying N , under isotropic scattering conditions for both the EMI and propagation channels $\{\mathbf{h}_1, \mathbf{h}_2\}$. This implies that \mathbf{R}_2 and \mathbf{R} are not asymptotically orthogonal. In agreement with Proposition 1, SNR/N converges quickly to the limit in (24), irrespective of the strength of the direct link. The results show once again that, with there is a direct link, the benefit of having an RIS decreases as N grows large (even if the β_d is relatively weak compared to $\beta_1 = \beta_2 = -55$ dB). This is not the case when EMI is neglected where using an RIS is always beneficial, even in presence of a direct link, e.g. [4, Fig. 5].

To quantify the impact of the spatial correlation matrices \mathbf{R}_2 and \mathbf{R} , we assume that the power spectral density of the channel vectors \mathbf{h}_i for $i = 1, 2$ is

$$f_i(\varphi, \theta) = \frac{c}{2\pi \bar{\sigma}_{i,\varphi} \bar{\sigma}_{i,\theta}} e^{-\frac{(\varphi - \bar{\varphi}_i)^2}{2\bar{\sigma}_{i,\varphi}^2}} e^{-\frac{(\theta - \bar{\theta}_i)^2}{2\bar{\sigma}_{i,\theta}^2}} \cos(\theta) \quad (27)$$

where c is a constant such that $\int_{-\pi/2}^{\pi/2} \int_{-\pi/2}^{\pi/2} f_i(\varphi, \theta) d\varphi d\theta = 1$. This represents a concentration of plane waves around the nominal angle pair $(\bar{\varphi}_i, \bar{\theta}_i)$ with a Gaussian angular distribution. We fix $\bar{\varphi}_1 = 0$, $\bar{\varphi}_2 = \pi/4$, $\bar{\theta}_1 = \pi/4$, $\bar{\theta}_2 = 0$ and $\bar{\sigma}_{1,\varphi} = \bar{\sigma}_{1,\theta} = \bar{\sigma}_{2,\varphi} = \bar{\sigma}_{2,\theta} = \pi/6$. The power spectral density $f(\varphi, \theta)$ of the EMI is modeled in the same way as (27) with fixed $\bar{\varphi} = -\pi/4$ and $\bar{\theta} = 0$, while $\sigma^2 = -60$ dB. Fig. 5 illustrates the SNR in (20) for a varying N , different values of $\bar{\sigma}_\varphi = \bar{\sigma}_\theta$. The SNRs with isotropic \mathbf{R} (given by (14)) and without EMI are also reported as references. The lowest SNR is achieved when

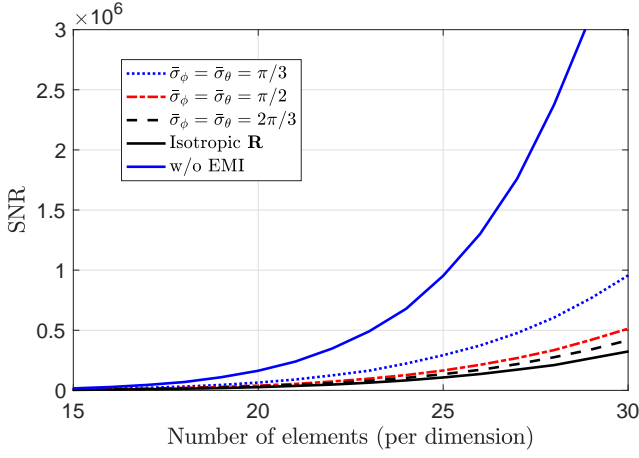


Fig. 5. Scaling behavior of the optimized SNR as a function of N for non-isotropic scattering for \mathbf{n} and $\{\mathbf{h}_i\}$ for $i = 1, 2$. The same parameters as in Fig. 4 with $\beta_d = -\infty$ dB is considered. The isotropic channel for EMI is also reported.

the EMI is isotropic. We see that the SNR increases as $\bar{\sigma}_\varphi = \bar{\sigma}_\theta$ reduces since the overlap between the domains of $f(\varphi, \theta)$ and $f_2(\varphi, \theta)$ decreases. Compared to the case without EMI, a large gap is observed even for the relatively small angular interval $\bar{\sigma}_\varphi = \bar{\sigma}_\theta = \pi/3$, for which the domains of $f(\varphi, \theta)$ and $f_2(\varphi, \theta)$ overlaps marginally. More importantly, for all the investigated scenarios, the SNR is far from scaling as in the case without EMI. All this is in agreement with Proposition 1.

Remark 2. The unbounded behavior of the SNR as $N \rightarrow \infty$ is not physically meaningful since we cannot receive more power than what was transmitted. Hence, there must be a finite upper bound on the SNR even when $N \rightarrow \infty$. In this letter, the unbounded behavior of the SNR is a consequence of the models in Section II-B and Section II-C, which are obtained under the classical far-field assumption. The latter breaks down when the RIS grows large. To ensure the convergence of the SNR towards a finite upper limit, the models must be refined to capture the geometric near-field properties, as $N \rightarrow \infty$; as done for example in [17] in the context of deterministic propagation conditions. That said, we stress that the importance of asymptotics is not to quantify the asymptotic performance limits but rather to gain insights into practical scenarios with a large but finite N (any practical RIS will be finite-sized). This is exactly how the asymptotic findings in Proposition 1 have been used in the setups of Figs. 4 and 5.

IV. CONCLUSIONS

RIS-aided communications will always operate in the presence of electromagnetic interference, unless in an anechoic chamber designed to completely absorb reflections of uncontrollable electromagnetic waves. We provided a physically meaningful model for the electromagnetic interference and used it to evaluate its impact on the end-to-end SNR of an RIS-aided communication system for operating in a random scattering environment. The analysis showed that EMI may have a severe impact, especially when the number of passive elements N grows large and/or when a strong direct link

is present. While the RIS can make the received signal power grow as N^2 , it will also reflect EMI power that is generally proportional to N . Hence, in the asymptotic regime as $N \rightarrow \infty$, the SNR grows as N . It is only in the case when the spatial correlation matrices of the electromagnetic interference and the channel from the RIS to the receiver are asymptotically orthogonal that the SNR will grow as N^2 , as reported in previous work that neglected the EMI.

The analysis considered an RIS that is optimized against thermal noise only, since the EMI statistics are hard to estimate in practice. It might be interesting to analyze if better performance can be achieved by tuning the RIS based on the statistical properties of the EMI.

REFERENCES

- [1] M. D. Renzo *et al.*, “Smart radio environments empowered by reconfigurable intelligent surfaces: How it works, state of research, and road ahead,” *IEEE J. Sel. Areas Commun.*, vol. 38, no. 11, pp. 2450–2525, 2020.
- [2] Q. Wu and R. Zhang, “Towards smart and reconfigurable environment: Intelligent reflecting surface aided wireless network,” *IEEE Commun. Mag.*, vol. 58, no. 1, pp. 106–112, 2020.
- [3] Q. Wu, S. Zhang, B. Zheng, C. You, and R. Zhang, “Intelligent reflecting surface-aided wireless communications: A tutorial,” *IEEE Transactions on Communications*, vol. 69, no. 5, pp. 3313–3351, 2021.
- [4] E. Björnson, H. Wymeersch, B. Matthiesen, P. Popovski, L. Sanguinetti, and E. de Carvalho, “Reconfigurable intelligent surfaces: A signal processing perspective with wireless applications,” 2021, Online: <https://arxiv.org/abs/2102.00742>.
- [5] Q. Wu and R. Zhang, “Towards smart and reconfigurable environment: Intelligent reflecting surface aided wireless network,” *IEEE Commun. Mag.*, vol. 58, no. 1, pp. 106–112, 2020.
- [6] —, “Intelligent reflecting surface enhanced wireless network via joint active and passive beamforming,” *IEEE Trans. Wireless Commun.*, vol. 18, no. 11, pp. 5394–5409, 2019.
- [7] C. Huang, A. Zappone, G. C. Alexandropoulos, M. Debbah, and C. Yuen, “Reconfigurable intelligent surfaces for energy efficiency in wireless communication,” *IEEE Trans. Wireless Commun.*, vol. 18, no. 8, pp. 4157–4170, 2019.
- [8] D. Middleton, “Statistical-physical models of electromagnetic interference,” *IEEE Trans. Electromagnetic Compatibility*, vol. EMC-19, no. 3, pp. 106–127, 1977.
- [9] S. Loyka, “Electromagnetic interference in wireless communications: behavioral-level simulation approach,” in *IEEE 60th Vehicular Technology Conference, 2004. VTC2004-Fall. 2004*, vol. 6, 2004, pp. 3945–3949 Vol. 6.
- [10] M. A. Jensen and J. W. Wallace, “Capacity of the continuous-space electromagnetic channel,” *IEEE Trans. Antennas Prop.*, vol. 56, no. 2, pp. 524–531, 2008.
- [11] E. Björnson and L. Sanguinetti, “Rayleigh fading modeling and channel hardening for reconfigurable intelligent surfaces,” *IEEE Wireless Commun. Lett.*, vol. 10, no. 4, pp. 830–834, 2021.
- [12] C. Huang, A. Zappone, G. C. Alexandropoulos, M. Debbah, and C. Yuen, “Reconfigurable intelligent surfaces for energy efficiency in wireless communication,” *IEEE Trans. Wireless Commun.*, vol. 18, no. 8, pp. 4157–4170, 2019.
- [13] Ö. Özdoğan, E. Björnson, and E. G. Larsson, “Intelligent reflecting surfaces: Physics, propagation, and pathloss modeling,” *IEEE Wireless Commun. Lett.*, vol. 9, no. 5, pp. 581–585, 2020.
- [14] Q. Wu and R. Zhang, “Beamforming optimization for wireless network aided by intelligent reflecting surface with discrete phase shifts,” *IEEE Trans. Commun.*, vol. 68, no. 3, pp. 1838–1851, 2020.
- [15] R. Couillet and M. Debbah, *Random Matrix Methods for Wireless Communications*. USA: Cambridge University Press, 2011.
- [16] L. Sanguinetti, E. Björnson, and J. Hoydis, “Toward Massive MIMO 2.0: Understanding spatial correlation, interference suppression, and pilot contamination,” *IEEE Trans. Commun.*, vol. 68, no. 1, pp. 232–257, 2020.
- [17] E. Björnson and L. Sanguinetti, “Power scaling laws and near-field behaviors of Massive MIMO and intelligent reflecting surfaces,” *IEEE Open J. Commun. Society*, vol. 1, pp. 1306–1324, 2020.